

Oral dysbiosis initiates periodontal disease in experimental kidney disease

David Randall¹, Asil Alsam², Julius Kieswich¹, Susan Joseph², Joseph Aduse-Opoku², Jonathan Swann³, Alan Boyde⁴, Graham Davis⁴, David Mills⁴, Kieran McCafferty¹, Michael Curtis² and Muhammed M. Yaqoob¹

¹William Harvey Research Institute, Queen Mary University of London, Charterhouse Square, London, UK

²Faculty of Dentistry, Oral and Craniofacial Sciences, King's College London, London, UK

³School of Human Development and Health, Faculty of Medicine, University of Southampton, Southampton, UK

⁴Dental Physical Sciences Unit, Queen Mary University of London, London, UK

Correspondence to: David Randall; E-mail: d.randall@qmul.ac.uk

ABSTRACT

Background and hypothesis. It is presently unclear why there is a high prevalence of periodontal disease in individuals living with chronic kidney disease. Whilst some have argued that periodontal disease causes chronic kidney disease, we hypothesized that alterations in saliva and the oral microenvironment in organisms with kidney disease may initiate periodontal disease by causing dysbiosis of the oral microbiota.

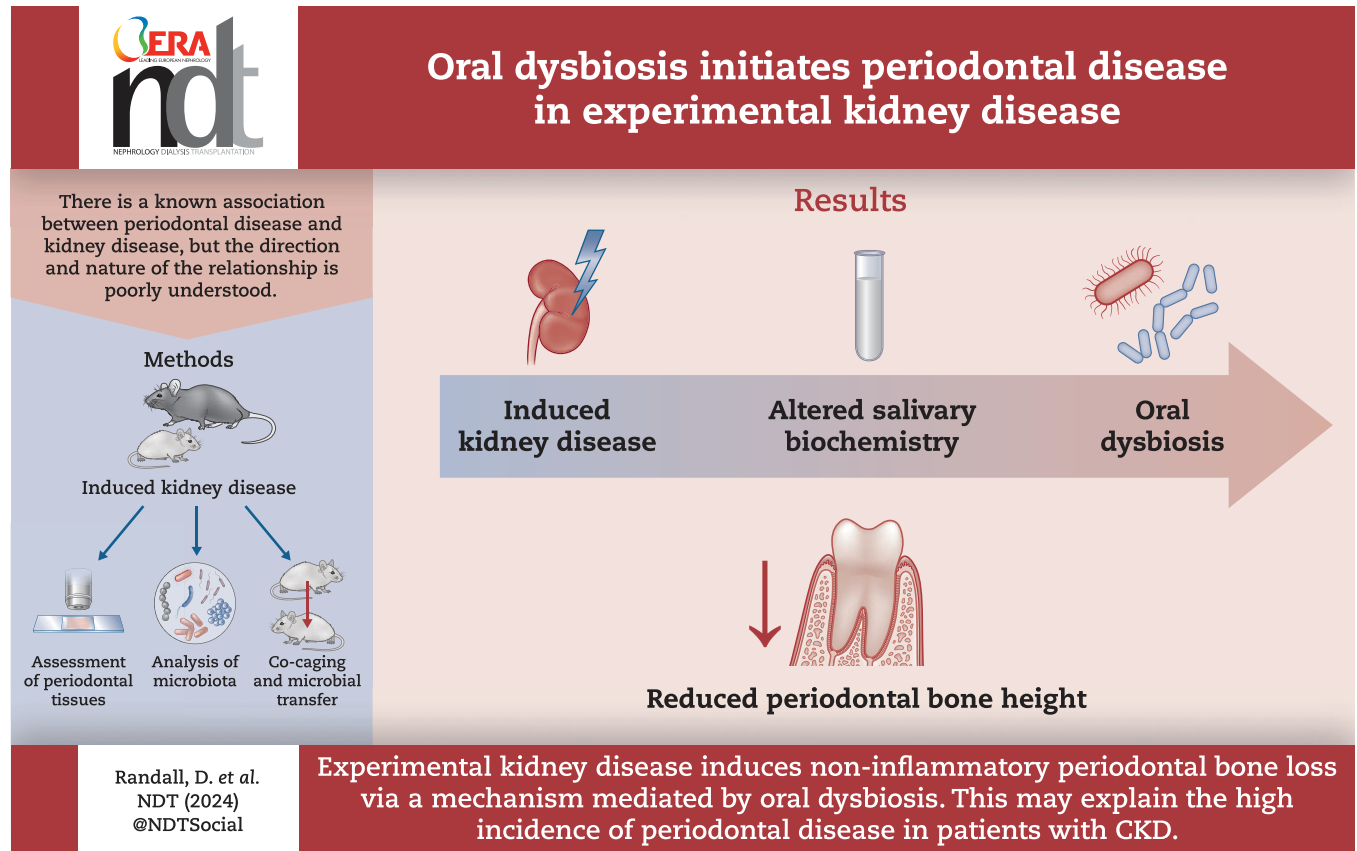
Methods. Experimental kidney disease was created using adenine feeding and subtotal nephrectomy in rats, and by adenine feeding in mice. Loss of periodontal bone height was assessed using a dissecting microscope supported by micro-CT, light, confocal and electron microscopy, and immunohistochemistry. Salivary biochemistry was assessed using NMR spectroscopy. The oral microbiome was evaluated using culture-based and molecular methods, and the transmissibility of dysbiosis was assessed using co-caging and microbial transfer experiments into previously germ-free recipient mice.

Results. We demonstrate that experimental kidney disease causes a reproducible reduction of alveolar bone height, without gingival inflammation or overt hyperparathyroidism but with evidence of failure of bone formation at the periodontal crest. We show that kidney disease alters the biochemical composition of saliva and induces progressive dysbiosis of the oral microbiota, with microbial samples from animals with kidney disease displaying reduced overall bacterial growth, increased alpha diversity, reduced abundance of key components of the healthy oral microbiota such as *Streptococcus* and *Rothia*, and an increase in minor taxa including those from gram-negative phyla *Proteobacteria* and *Bacteroidetes*. Co-housing diseased rats with healthy ones ameliorates the periodontal disease phenotype, whilst transfer of oral microbiota from mice with kidney disease causes periodontal disease in germ-free animals with normal kidney function.

Conclusions. We advocate that periodontal disease should be regarded as a complication of kidney disease, initiated by oral dysbiosis through mechanisms independent of overt inflammation or hyperparathyroidism.

Keywords: dysbiosis, experimental kidney disease, microbiome, oral microbial transfer, periodontal disease

GRAPHICAL ABSTRACT



KEY LEARNING POINTS

What was known:

- There is a high prevalence of periodontal disease in patients with chronic kidney disease.
- The nature, direction, and causative relationship underlying this association is poorly understood.

This study adds:

- Induced kidney disease causes reduced periodontal bone height in rodent models.
- We demonstrate a potential mechanism, with kidney disease altering salivary biochemistry and inducing oral dysbiosis.
- Co-housing and microbial transfer experiments suggest that dysbiosis may have a causative role in the periodontal bone loss seen in the context of kidney disease.

Potential impact:

- Periodontal disease should be viewed as a complication of chronic kidney disease.
- This may suggest that dental care be included in the routine management of patients with chronic kidney disease.
- The implication of bacteria in the pathogenesis of periodontal disease requires further study, but may suggest novel opportunities for treatment.

INTRODUCTION

Periodontal disease (PoD) is a complex pathological process in which a bacterial challenge presented by a dysbiotic microbial community in subgingival dental plaque [1] drives a deregulated immune and inflammatory response that ultimately causes osteoclastic resorption of alveolar bone and eventual loss of teeth [2].

Patients living with chronic kidney disease (CKD) have a high prevalence of PoD [3–5], and some have suggested that chronic,

low-level inflammation caused by PoD may lead to progressive renal dysfunction and increased cardiovascular disease [6, 7].

However, there are several reasons to support the view that CKD may actually cause PoD. Patients with CKD have abnormalities in the flow rate and biochemical composition of saliva [8, 9], altering the oral microenvironment and exerting selective pressure on the resident microbiota. Furthermore, patients with CKD suffer abnormalities of bone metabolism [10] and impaired immune function [11], which may also be relevant to the development of PoD.

We hypothesized that CKD may be a cause of PoD, reversing current understanding of the association between these conditions, and that induction of dysbiosis of the oral microbiota may be a critical mechanism in this process.

MATERIALS AND METHODS

Animal work

Study approval

Animal experiments were conducted in accordance with the UK Home Office Animals (Scientific Procedures) Act 1986, with local ethical committee approval. All animal work was carried out in the Biological Services Unit of Queen Mary University of London (QMUL) at Charterhouse Square, and complied fully with all relevant animal welfare guidance and legislation (UK Home Office Project License number PPL 70/8350).

Sex as a biological variable

Male animals were used throughout because of the potential for female reproductive hormones to influence the kidney disease phenotype or introduce phenotypic heterogeneity into the study population. The generalizability of these data to mixed human populations is discussed.

Number of animals used

A total of 48 rats and 35 mice were used in the experiments described. Samples sizes were determined by prior experience within our group; no formal power calculations were employed. Data from all animal subjects were included in the analysis; none were excluded on the basis of animal phenotype or results. Data from individual animals was excluded from specific analyses (e.g. microbiome analysis or histology) where it did not meet quality standards as set out in individual sections below (e.g. where PCR from individual swabs did not achieve sufficient amplification for meaningful analysis). There was no formal randomization into intervention and control groups and researchers were not blinded to group allocation.

Source of animals

All rats used in the experiment were male, outbred Wistar IGS rats obtained from Charles Rivers (Kent, UK) at 7 weeks of age. All were housed in individually ventilated cages under 12 h light/dark cycles and were allowed unlimited access to water and feed (RM1 diet, or RM1 with 0.75% adenine, from Special Diet Services, Essex, UK).

All mice used in the experiment were male, wild-type C57BL/6 mice. Those used in the adenine feeding experiment were obtained from Charles Rivers at 7 weeks of age, whilst germ-free mice of the same species were obtained from a colony maintained by one of the authors (M.C.) at the Biological Research Facility, St George's University of London, at 8 weeks of age. All were housed in individually ventilated cages under 12 h light/dark cycles and were allowed unlimited access to water and diet (RM1 diet or RM1 + 0.15% adenine, from Special Diet Services, Essex, UK).

Chemically induced kidney disease in rats

The total cohort size was 18 rats. After a week-long period of acclimatization, nine rats were started on the adenine-containing intervention diet whilst another nine were maintained on a standard control diet. This diet was continued for 4 weeks, followed by a washout period of 4 weeks when all animals received the control diet, after which the animals were sacrificed. Oral swabs were

taken from all animals at the point of maximal kidney injury for those receiving the intervention diet (at the end of the 4-week period of adenine administration). Serum samples were obtained by thoracotomy at the point of sacrifice, and other tissues were obtained as outlined below.

Surgically induced kidney disease in rats

The total cohort size was 24 rats. After a week-long period of acclimatization, 14 underwent subtotal nephrectomy (SNx), involving exteriorization of the left kidney with decapsulation and removal of the upper and lower poles and subsequent replacement of the middle pole only, followed by total right nephrectomy 2 weeks later. Ten underwent sham procedures, involving exteriorization, decapsulation and replacement of the left kidney, followed by the same procedure on the right kidney 2 weeks later. Oral swabs to assess the microbiota were taken 4 weeks after the second stage of the surgical procedure to parallel those taken in the chemically induced kidney disease protocol. A 24-hour urine collection was performed in the week prior to sacrifice (results from this have been published elsewhere [12]).

Animals in these cohorts were used in the co-housing experiment: from 2 weeks after the second stage of surgery, 11/24 animals continued to be housed in individually ventilated cages with other animals that had undergone the same surgical procedure (SNx with SNx or sham with sham; the other 13 were co-housed [SNx with sham]) (described in Fig. 2F), to examine whether this affected microbiological or periodontal parameters.

Additional rats for histological and salivary analysis

Twelve additional rats were used in order to obtain saliva samples for subsequent analysis, and to undertake bone staining to assess the bone formation rate. These rats underwent SNx or sham procedures as outlined above ($n = 6$ sham surgery, $n = 6$ SNx), and were otherwise looked after identically to those in the 'Surgically induced kidney disease in rats' protocol above. In their final week of life, 500 μ g calcein green (approximately 1 mg/kg) was injected intravenously three times at exact 48 h intervals. The following week induced saliva collection was carried out under terminal anaesthesia with ketamine/xylocaine. After full induction of anaesthesia, 1 mg pilocarpine was injected into the peritoneum, with a further 1 mg administered 5 minutes later if there was no salivary response. Saliva was then collected over the following 8 minutes using a 100 mL pipette and 1.5 mL Eppendorf tubes. Salivary volume was directly assessed by weighing the filled tubes and subtracting the weight of the tube itself. Salivary pH was directly measured using a pH meter and narrow gauge probe (Mettler Toledo, Leicester, UK), before saliva was snap frozen in liquid nitrogen and transferred to a -80° freezer until the time of analysis.

Chemically induced kidney disease in mice

The total cohort size was 20 mice. After a week-long period of acclimatization, 10 animals were placed on an intervention diet (RM1 with 0.15% adenine), whilst 10 remained on standard RM1 diet. Oral swabs to assess changes in microbiota were obtained at age 7 weeks, 10 weeks, 14 weeks, 18 weeks, 22 weeks, and 26 weeks of age—i.e. prior to starting the experimental protocol, and at 2 weeks, 6 weeks, 10 weeks, 14 weeks, and 18 weeks after starting it. All mice were sacrificed at age 28 weeks after a 24-hour urine collection. Additional oral swabs were obtained prior to the time of sacrifice from four 'donor' animals in each group, for using in the 'oral microbial transfer' experiment described below. Additionally, soiled cage contents including bedding and droppings

from the cages in which these donor animals were housed, were frozen for further use as described below.

Additional mice for histological analysis

Jaw samples from a previous cohort of male, wild-type C57BL/6 mice, treated identically to those described above, were processed for histological examination.

Oral microbial transfer in mice

Fifteen germ-free C57BL/6 mice were transferred direct from their sterile isolator at the Biological Research Facility, St George's University of London, to the Biological Services Unit at Charterhouse Square using a clean but non-sterile specialist animal transfer company (Impex, UK) in three separate batches (one batch of seven for receipt of microbiota from control donors, two batches of four each for receipt of microbiota from kidney disease donors).

On arrival, each mouse received oral microbial transfer (OMT) by oral gavage of swabs taken from donor animals as described above. Each donor swab was used to transfer into two (or in one case, one) recipient(s); seven were designated control recipients and eight, kidney disease recipients. Gavage was carried out by using a sterile swab thoroughly immersed in transport medium that had been frozen since the time of sampling, and agitating the swab in the mouth of the recipient mouth for 15 seconds and encouraging them to suck on it. After receiving the OMT, the mice were placed in cages containing cage contents from the cage occupied by the particular donor animals, which had been frozen at -80° until the time of use, to permit ongoing microbial transfer by coprophagy.

Animals were then maintained in ordinary individually ventilated cages in an open area of the Biological Services Unit, with standard 12-h light/dark cycles. They had unlimited access to standard RM-1 diet and tap water. Oral swabs were taken to assess the efficacy and durability of bacterial transfer at 3 weeks and 9 weeks after transfer in all animals, and all animals were then culled, after a 24-hour urine collection, at 18 weeks of age (10 weeks after transfer).

Laboratory methods

Processing of blood samples

Animals in all experimental groups were sacrificed by lethal injection of sodium thiopentone (LINK Pharmaceuticals, Horsham, UK). Blood samples were obtained by thoracotomy and cardiac puncture, and spun down directly to isolate serum, which was frozen at -80° until the time of analysis. Quantification of serum urea, creatinine, calcium, and phosphate concentrations was done by IDEXX Bioresearch, Ludwigsberg, Germany. Serum parathyroid hormone concentrations were assessed using a PTH ELISA kit suitable for rat serum (RayBiotech), used according to the manufacturer's instructions.

Measurement of alveolar bone height

The primary outcome measure to define periodontal disease was macroscopic evidence of loss of alveolar bone height. Heads were removed and jaw specimens obtained from all animals using a guillotine and sharp dissection with scissors. Alveolar bone height was measured using a morphometric method previously demonstrated to have equal reliability to radiological [13] and histological techniques [14]. After any samples (typically mandibles) required for conventional histology, micro-CT or scanning electron microscopy were removed, skulls were chemically defleshed by incubation in the protease-based detergent Terg-a-zyme® (Sigma-

Aldrich, UK), for 48 hours at 55°C , with remaining soft tissue being removed mechanically after this. One of the authors (A.A.) who has significant expertise in the procedure obtained photographs using a dissecting microscope and measured the distance between the cemento–enamel junction and the alveolar bone crest using ImageJ software [15], as outlined by Baker and colleagues [16], although without the use of blue dye. Bone height was measured over the lingual and buccal surfaces of each molar root, a total of four measurements for each of twelve molars, yielding a total of 48 measurements for each animal from which the mean bone loss for each animal was calculated. These figures are expressed relative to the average bone height in control animals, with significance assessed using Student's t-test with Welch's correction for unequal variances.

Light microscopy

Tissues removed prior to defleshing were fixed in formalin, decalcified using 10% formic acid (rats samples) or EDTA (mouse samples), and embedded in paraffin. The molar teeth were sectioned at $5\ \mu\text{m}$ in a frontal (buccolingual) orientation. Every tenth section was stained by haematoxylin and eosin using an automated slide processor, and then photographed using the Pannoramic 250 FLASH III 2.0 slide imaging system.

Immunohistochemistry

Immunohistochemistry was carried out at the Barts Cancer Institute using the Ventana Discovery XT system using primary antibodies against IL-17 and neutrophil defensin 4 (Abcam, Cambridge, UK) and tartrate resistant acid phosphatase (Insight Biotech). Sections were then viewed and photographed using the same slide imaging equipment as used for light microscopy of the H&E stained slides.

Scanning electron microscopy

Samples were transported in 70% ethanol to the Dental Physical Sciences Unit at the Mile End Campus, QMUL. Some samples were rendered anorganic by treatment with 7% available chlorine sodium hypochlorite bleach for 3 weeks to remove all soft tissue. This treatment completely removes the periodontal ligament so that the teeth could be removed manually to expose the surface of the alveolar bone. All SEM imaging was done using 20 kV accelerating voltage and a solid state backscattered electron (BSE) detector, using a chamber pressure of 50 Pa in a Zeiss EVO MA10 scanning electron microscope.

Confocal scanning light microscopy

Samples in 70% ethanol from calcein-injected animals were then embedded in polymethyl methacrylate (PMMA), and blocks were cut and polished to produce flat surfaces before being used for confocal scanning light microscopy (CSLM). CSLM was carried out at the Rockerfeller Building, Division of Biosciences, University College London using a Leica SPE confocal system with an inverted microscope. The PMMA blocks were cover-slipped with glycerol. Objectives used were 10/0.45, 20/0.75, and 63/1.3 oil. Images were analysed using ImageJ software and a measure of the daily rate of dentine and bone formation calculated at the incisor root and lower mandibular border, respectively. The bone formation rate (BFR) was calculated using the formula $\text{BFR} = \text{MAR} \times (\text{MS/BS})$ as suggested by the ASBMR Histomorphometry Nomenclature Committee [17], where the mineral apposition rate (MAR) was calculated by dividing the distance between the innermost and outermost calcein bands (given 96 h apart) by four, and the

mineralizing surface (MS) and bone surface (BS) were measured directly using ImageJ.

Micro CT

This was carried out on samples embedded in PMMA. Samples were scanned on the MuCAT2 micro-CT system designed and operating in the Dental Physical Sciences unit at the Mile End Campus, QMUL. The samples were scanned at 90 kV and 180uA at 20 or 22um voxel size. Reconstruction was performed with GPU accelerated filtered Feldkamp backprojection algorithm and the grey-level data was calibrated to linear attenuation coefficient at 40 keV using a multi-material calibration carousel and X-ray modelling software [18]. Quantification of bone mineral density was carried out by assessing the mean linear attenuation coefficient of 20 tagged regions with a radius of three pixels in three dimensions at each tagged location and a calibration voltage of 27.5 keV.

Collection of samples for analysis of oral microbiota

Oral swabs were taken from animals at the timepoints described above by agitating sterile cotton swabs against the molars of rats or mice being held in the scruff position for a period of 30 seconds. Swabs were then placed into 100 µl transport medium and transferred directly to the laboratory, where they were vortexed for 30 seconds to mobilize cells and 30 µl was removed for culture. The remaining transport medium and swab was frozen at -80°C for subsequent DNA extraction.

Culture analysis

Transport medium withdrawn for culture was serially diluted and spread onto blood agar plates containing 5% defibrinated horse blood (TCS Biosciences, UK) before being incubated under both aerobic and anaerobic conditions (80% N₂, 10% H₂, and 10% CO₂) for 48 hours at 37°C. After this, colonies were counted according to morphology and grown to purity on new blood agar plates. DNA was extracted using the GenElute Bacterial Genomic DNA extraction kit (Sigma Aldrich, UK). PCR products were cleaned up using the NucleoSpin® Gel and PCR clean-up kit (Machery-Nagel, Germany), and then identified using Sanger sequencing of the whole 16S rRNA gene (Eurofins Scientific, Luxembourg), using the widely used 27F-1492R primer pair, which have been used previously by our group to identify cultured oral microbes [19, 20]. Consensus sequences of forward and reverse reads were assembled using the BioEdit Sequence Alignment Editor [21], and full length 16S rRNA gene sequences were assembled from forward and reverse reads using the CAP3 Contig Assembly Programme [22] available online via the Pôle Rhône-Alpes de Bioinformatique Site (<http://doua.prabi.fr/software/cap3>). All consensus sequences were >1400 base pairs in length and the mean length was 1456 bp.

Additional in vitro bacterial work

In vitro assessment of urease activity and tolerance of variable urea concentrations were assessed for all bacterial isolates after they were grown to purity on 5% blood agar plates under standard aerobic or anaerobic conditions.

Urease activity was assessed in all isolates by culturing under either aerobic or anaerobic conditions on Christensen's urea agar (Sigma-Aldrich) at 37°C. A positive urease result was recorded if there was a colour change to purple, and the sample was re-grown if there was no discernable growth on the top of the agar.

Two broths were used in order to assess bacterial growth at different concentrations of urea: Iso-sensitest broth (ThermoFisher Scientific) and Brain-Heart Infusion (BHI) broth (SigmaAldrich).

The BHI broth was used for some samples after they could not be grown after several attempts in Iso-sensitest broth. One isolate (identified as *Haemophilus parainfluenzae*) did not grow in either broth, and after researching its specific growth requirements in the published literature, eventually grew well after filter-sterilized hemin and nicotinamide adenine dinucleotide were added to the growth medium.

Preparations of both broths were prepared at variably stronger concentrations than the manufacturer's instructions would suggest so that when diluted with different concentrations of filter-sterilized 60% urea solution, broths with eventual concentrations of 0%, 4%, 8%, 12%, 18%, and 24% urea were created.

Bacteria grown to purity on blood agar were then transferred into 2 ml sterile phosphate buffered saline (PBS). A 1 ml aliquot was assessed using a spectrophotometer at 600 nm and the remainder of the bacterial solution further diluted with sterile PBS to achieve a standard turbidity of 0.5 McFarland units, equating to a concentration of bacteria of 1.5×10^8 colony forming units/ml (cfu/ml). These solutions were further diluted 50-fold to achieve an approximate concentration of 3×10^6 cfu/ml, and then 34 µl of this bacterial preparation were added to 200 µl of varying concentrations of urea broth in a 96-well plate, to achieve 234 µl incubations each containing approximately 5×10^5 cfu bacteria in eventual urea concentrations of 0%, 3.3%, 6.6%, 10%, 15%, and 20%.

These plates were then incubated at 37° in either aerobic or anaerobic conditions for 24 hours before being read on a plate reader at 620 nm. The mean inhibitory concentration was defined for each organism as the urea concentration at which the optical density of the solution was decreased to less than 10% of the difference between 0% urea and control (non-inoculated) wells. One isolate did not achieve sufficient growth to allow calculation of MIC.

DNA extraction and PCR for next-generation sequencing

The remaining transport solution not used for culture analysis, along with the swab, was transferred to bead beating tubes from the DNeasy PowerSoil kit from QIAGEN, used according to the manufacturer's instructions including an 8-minute bead-beating step using the FastPrep-24™ homogenizer (MP Biomedicals). All samples were processed using the same kit, and negative 'kitome' control samples were included for each extraction kit used [23]. PCR was carried out using barcoded 27F/338R primer pairs, targeting the V1/V2 hypervariable region of the 16S rRNA gene. PCR was carried out in a sterile 96-well plate using Phusion Green Hot Start II High Fidelity PCR Master Mix (ThermoFisher Scientific), using an initial denaturation step for 5 mins at 98°C followed by 25 cycles of 98°C for 10 s, 53°C for 30 s, 72°C for 45 s, and a final extension of 72°C for 10 min.

Next generation sequencing

Normalization of DNA concentrations was carried out using SequalPrep™ Normalisation Plates (ThermoFisher) and DNA was quantified using either the Quant-iT® PicoGreen™ dsDNA Quantitation Kit (ThermoFisher Scientific) or a Qubit® 4 Fluorometer (also ThermoFisher). The samples were pooled and sequenced in two runs; one at the Barts and the London Genome Centre, QMUL; and one in the DNA Sequencing Facility, in the Department of Biochemistry at the University of Cambridge; each using an Illumina MiSeq 2 × 250 flow cell for paired-end sequencing.

Quantification of salivary urea

A colorimetric detection kit for urea nitrogen (ThermoFisher Scientific) was used according to the manufacturer's instructions.

Samples of saliva were processed at 1:2 and 1:20 dilutions and the mean concentration using both dilutions in duplicate was accepted. Corresponding serum samples were analysed using the same kit but at 1:20 and 1:40 dilutions to allow comparison.

NMR spectroscopy of saliva

Saliva samples were diluted with buffer containing trimethylsilylpropanoic acid (TSP) and analysed on an NMR spectrometer (Bruker) operating at 600.22 MHz ^1H frequency at Imperial College London.

Statistical methods

Statistical analysis of bone height data

All data for loss of periodontal bone height was found to be normally distributed when assessed by the Shapiro-Wilk test. All testing for significance of difference between two groups was carried out using Student's t-test with Welch's correction for unequal variances, in GraphPad Prism and Microsoft Excel.

Analysis of effect of housing on microbiology and bone height

Two-way ANOVA was carried out in GraphPad Prism to define the significance of the different levels of bone loss (dependent variable), according to both housing and treatment class (independent variables) in the surgically induced kidney disease experiment. No comparable analysis was carried out for the chemically induced kidney disease protocol because it was impossible to vary the housing since all animals in a single cage received the same diet.

Analysis of urea tolerance

The proportional increased average growth per sample in kidney disease versus control animals was plotted (shown in Fig. 3B), calculated as (mean growth in kidney diseases/mean growth in controls) where the mean growth in kidney diseases was higher than that in controls; and as (mean growth in controls/mean growth in kidney diseases) where the mean growth in controls was higher.

Linear regression was used to draw a line of best fit between the mean inhibitory concentration of urea and the relative competitiveness of different isolates in control versus kidney disease animals (presented in Fig. 4B); standard settings in GraphPad Prism were used to accomplish this and Prism software was used to calculate the slope and the significance of its gradient.

Identification of cultured bacterial isolates

Isolates were identified by comparing their 16S rRNA gene sequences with reference datasets using both the NCBI Nucleotide BLAST database (<https://blast.ncbi.nlm.nih.gov/Blast.cgi>), and the Ribosomal Database Project (RDP) [24] online search tool (<https://www.glbrc.org/data-and-tools/glbrc-data-sets/ribosomal-database-project>). In many cases these tools agreed on a species-level identification for the isolate, but in some cases agreement between the two was only at higher taxonomic levels (such as in the case of different species of *Streptococcus* or *Enterobacteriaceae*). Thus, for all isolates, full-length reference 16S rRNA gene sequences for all species within the genus identified by BLAST and RDP search were downloaded from the RDP Hierarchy Browser. These reference sequences were aligned with the sequences from our research isolates, trimmed to a uniform length and used to construct a maximum likelihood tree, using MEGA [25] version 7. Pairwise distances between all isolates within a

particular genus and all reference sequences within that genus were calculated and used to generate a distance matrix.

Species-level identification was determined when possible at >98.5% sequence identity. Isolates that failed to obtain any match at this level were treated as potential novel species. One was a *Streptococcus* species (four isolates) with a closest proximity to *S. danieliae* at 97.33%, and another was a *Pasteurella* species (closest match being *P. pneumotropica* at 94.7%).

Analysis of cultured microbiota data

Once assigned a species identity, the abundance of each isolate (\log_{10} of colony forming units/ml) was carried out using Microsoft Excel and GraphPad Prism, using the Student t-test with Welch's correction to assess difference between growth in kidney disease animals and growth in controls. Comparisons were made at species level and then aggregated to allow comparisons at higher taxonomic levels.

Handling of isolates with regard to statistical analysis of in vitro culture data

For the purposes of in vitro microbiological work (urease testing and calculation of the mean inhibitory concentration of urea), where more than one isolate was assigned to a particular species identity, differences in in vitro characteristics were resolved for subsequent analysis by treating all isolates assigned to one species as urease positive if one isolate of that species was urease positive, and all isolates within a single species identification as possessing the highest urea tolerance of any isolate in that species.

Processing of 16S sequencing data

Sequence data were processed using the DADA2 pipeline [26] in R, according to the author's recommended protocol (available from https://benjjneb.github.io/dada2/tutorial_1_6.html), adjusting filter parameters to achieve maximum quality scores whilst achieving sufficient overlap between forward and reverse read. Sequences were aligned against Silva v128 [27] in order to assign taxonomy.

Raw abundance data of sequence variants were used with taxonomic assignments and sample metadata to create phyloseq [28] objects. Phylogenetic trees were generated using MEGA v7.0, and rooted to a random node using the R package *phytools* [29]. A pseudocount of 0.001 was added to all OTU abundances to avoid calculating log-ratios involving zeros, and data was then made compositional through isometric log-ratio transformation using the R package *philr* [30]. Ordination was carried out using the 'ordinate' function in *Phyloseq*, based on Euclidean distances in *philr* space. Permutational analysis of variance (PERMANOVA) and the PERMDISP test for homogeneity of variance (as proposed by Anderson [31]), were carried out using the R package *vegan* [32]. Alpha diversity was assessed using *Phyloseq*. Compositional analysis of the microbiota at six taxonomic levels was based on isometric log-ratio transformation of raw sequence abundances and adjusted for multiple testing using the Benjamini-Hochberg method, carried out using the ANCOM statistical framework [33] in R, with code obtained from the author's webpage: <https://sites.google.com/site/siddharthamandal1985/research>.

Analysis of NMR spectral data

NMR spectral profiles were digitized and imported into Matlab (Mathworks). The peaks for water, urea, and TSP were excised from the raw NMR spectra, which were then aligned to adjust for variation in peak shift due to pH differences. Further

normalization was carried out using the Probabilistic Quotient method between samples in order to ensure comparable baselines between samples.

Positive identification of eight metabolites achieved by identifying their spectral profiles and confirming this using Chenomx NMR Suite 8.3 evaluation version (Chenomx, Edmonton, Canada), and peak integrals were calculated from metabolite peaks. Comparisons between these integrals were used to calculate differences in relative abundance using Microsoft Excel, with the Student's t-test and Welch's correction used to assess significance.

Preparation of figures

In order to achieve uniformity, all figures were generated using GraphPad Prism 7 (GraphPad Software Inc., San Diego, California).

RESULTS

Experimental kidney disease causes reduction in alveolar bone height without evidence of gingival inflammation

Renal impairment was induced in male Wistar rats using two protocols: chemically induced kidney disease (using adenine-containing feed) and surgically induced kidney disease (using SNx; for phenotypic and biochemical data on these animals see [Supplementary data S1](#)). Examination of de-fleshed heads revealed that rats with kidney disease generated using both experimental protocols displayed significant reductions in alveolar bone height compared with controls (an average of 0.113 mm less alveolar bone height relative to controls, $P < 0.0001$, Fig. 1A, B; [Supplementary data S1](#)). Kidney disease was then induced in wild-type C57-BL6 mice by administration of adenine-containing feed over a 20-week period; these animals also displayed reduced alveolar bone height compared with controls (-0.02 mm relative to the mean of controls, $P = 0.0005$; [Supplementary data S2](#)).

Histological examination of representative rat samples confirmed loss of alveolar bone height, but did not reveal the florid cellular gingival infiltrates seen in inflammatory periodontal disease (Fig. 1C, [Supplementary data S3](#)). Samples from mice were similarly devoid of overt inflammatory changes ([Supplementary data S4](#)). Immunohistochemistry using antibodies against IL-17 and neutrophil defensin 4 did not reveal any evidence of an inflammatory response in the gingival tissues in either rat or mouse samples. Staining against tartrate-resistant acid phosphatase (TRAP) did not demonstrate an increase in osteoclast numbers, suggesting that the reduced bone height may not be primarily caused by osteoclastic reabsorption ([Supplementary data S3](#)). Instead, scanning electron microscopy revealed striking differences in bone formation at the growing margins of the periodontal bone: whereas specimens from control animals demonstrated a 'spiky' bone surface, with evidence of Sharpey fibre formation, which precedes subsequent mineralization in healthy bone growth, specimens from kidney disease animals had a 'weathered' appearance almost devoid of Sharpey fibres, suggestive of a failure of bone growth at this surface (Fig. 1D and [Supplementary data 5](#)). Micro-computed tomography demonstrated abnormalities of bone formation in more recently deposited alveolar bone in kidney disease specimens, with a non-significant trend towards reduced mineral density (the linear attenuation coefficient in bone just below the alveolar bone crest was 1.604 cm⁻¹ in controls and 1.547 cm⁻¹ in kidney disease animals, $P = 0.069$; at sites deeper within the mandibular bone was 1.658 cm⁻¹ in controls and 1.621 cm⁻¹ in kidney disease animals, $P = 0.271$, Fig. 1E and [Supplementary data S6](#)).

To assess global rates of bone and tooth formation, samples from animals injected with three doses of 1 mg/kg calcein green at 48-hour intervals the week prior to sacrifice were assessed by confocal microscopy to calculate the daily rate of bone and tooth formation. Staining at the periodontal crest was highly variable and it was impossible to calculate a clear measure of bone formation rate, although many samples from kidney disease animals displayed ragged and irregular bone growth (Fig. 1F, [Supplementary data S7](#)). There were no differences between groups in the rate of tooth formation (the rate of dentine formation in the incisor was 14.78 $\mu\text{m}^3/\mu\text{m}^2/\text{d}$ in sham-operated controls vs 15.69 $\mu\text{m}^3/\mu\text{m}^2/\text{d}$ in SNx, $P = 0.517$), or the rate of bone apposition at the lower mandibular border, well away from the gingival tissues (4.249 $\mu\text{m}^3/\mu\text{m}^2/\text{d}$ in controls vs 3.562 $\mu\text{m}^3/\mu\text{m}^2/\text{d}$ in SNx, $P = 0.397$, [Supplementary data S7](#)), suggesting that the reduced height of alveolar bone, attributed to a failure of bone growth, is perhaps uniquely present in the growing periodontal bone.

To evaluate systemic features of CKD that may affect periodontal bone formation, we measured serum concentrations of parathyroid hormone (PTH), calcium, and phosphate. There was no difference in serum PTH concentrations between control and kidney disease animals (serum PTH 16.95 pg/ml in controls vs 12.37 in kidney disease animals, $P = 0.251$), or in serum calcium (2.58 mmol/L in controls vs 2.586 in kidney disease animals, $P = 0.841$) or serum phosphate (2.19 mmol/L in controls vs 2.107 in kidney disease animals, $P = 0.254$; [Supplementary data S1](#)).

Kidney disease is associated with oral dysbiosis

Oral swabs were assessed using both bacterial culture and next generation sequencing of the 16S rRNA gene amplicon to assess the effect of experimental kidney disease on the oral microbiota.

Lower total bacterial counts after 48 hours of incubation under both aerobic and anaerobic conditions were seen in samples from kidney disease animals (\log_{10} 6.07 cfu/ml transport medium in controls vs 5.80 in kidney disease, $P = 0.034$, Fig. 2A and [Supplementary data S8](#)), partly accounted for by substantially reduced total counts of the most abundant phylum, *Firmicutes* (\log_{10} 5.88 cfu/ml in controls vs 5.42 in kidney disease, $P = 0.043$). Conversely, absolute counts of Gram-negative phylum *Proteobacteria* were actually non-significantly higher in kidney disease animals than in controls (\log_{10} 4.12 cfu/ml in controls vs 4.55 in kidney disease, $P = 0.151$), which in the context of reduced overall counts in these animals meant that these kidney disease animals had significantly higher proportional abundances of *Proteobacteria* (9.53% vs 2.99% of total cultured bacteria, $P = 0.003$, Fig. 2B).

At genus level, kidney disease animals demonstrated lower counts of both the most abundant genus *Streptococcus* (\log_{10} 5.56 cfu/ml in controls vs 5.05 in kidney disease, $P = 0.017$), and the second most abundant genus *Rothia* (\log_{10} 5.56 cfu/ml in controls vs 5.23 in kidney disease, $P = 0.022$). Conversely, samples from kidney disease animals displayed higher growth of a number of minor taxa compared with control samples, which reached significance for the genus *Acinetobacteria* (\log_{10} 3.79cfu/ml in kidney disease, absent in controls, $P = 0.006$, Fig. 2C).

Next-generation sequencing of the 16S rRNA gene amplicon was used to confirm the pattern seen in the cultural analysis. Although the shorter read length obtained by using Illumina sequencing does not allow confident identification of organisms at lower taxonomic levels, the proportional abundances of different phyla plotted for each sample showed a similar decrease in

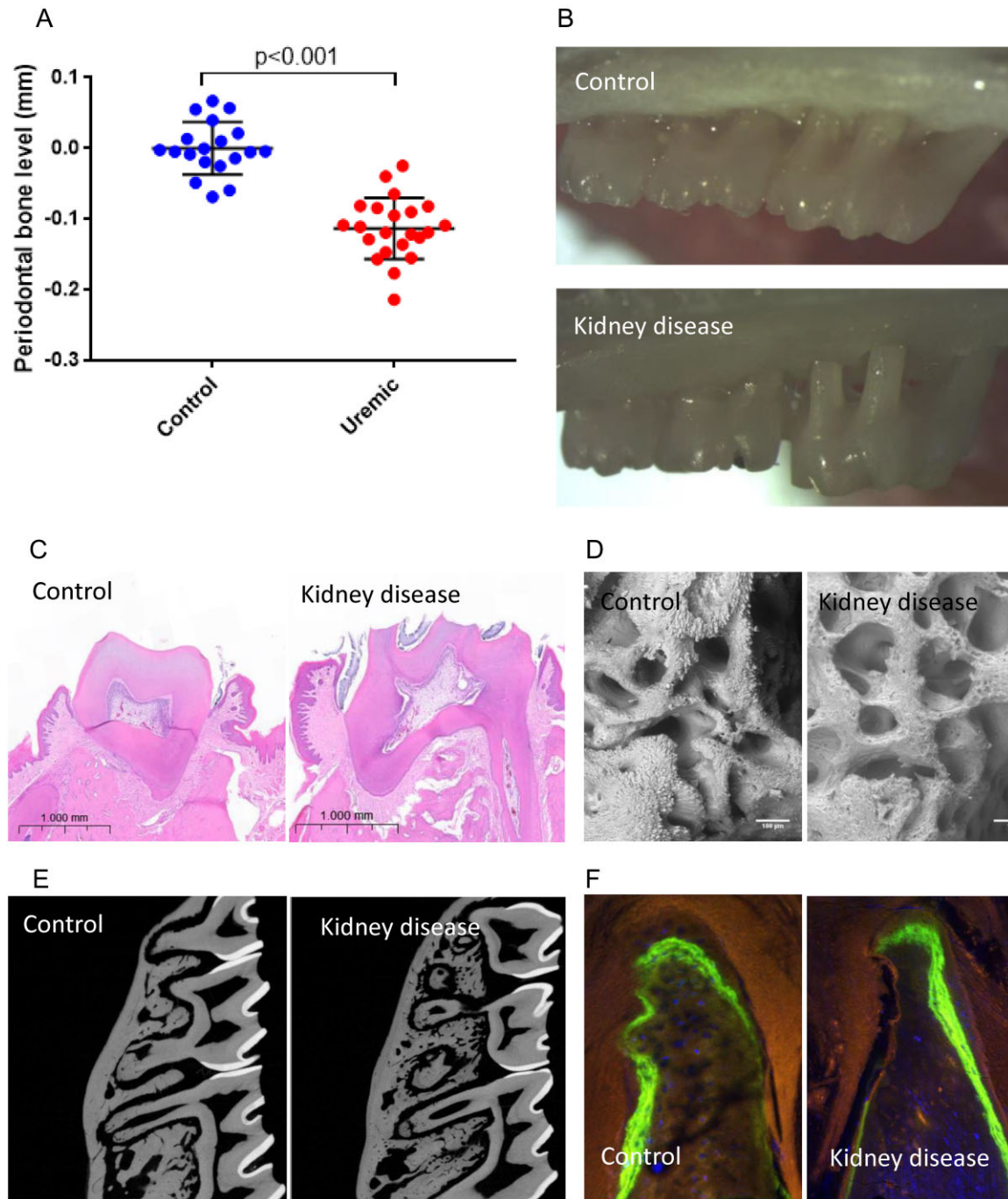


Figure 1: Experimental kidney disease causes periodontal disease. (A) Periodontal bone height in rats. Each point represents the average of multiple measurements over the buccal and lingual surfaces of all molar roots in a single rat, expressed relative to the average amount of bone height in all control animals. (B) Representative images showing lower maxillary alveolar bone height in a uraemic animal (bottom) compared with a control animal (top), visualized using a dissecting microscope at 20 \times magnification. The absence of alveolar bone is so significant in the uraemic animal that a clear gap can be seen between some of the roots and the bone crest. (C) Light microscopy of haematoxylin and eosin (H&E) stained slides of periodontal tissue using a 50 \times objective lens. (D) Scanning electron micrographs of the surface of alveolar bone facing the periodontal ligament and tooth roots in macerated specimens. (E) Micro-computed tomography in the para-sagittal plane through the molar roots. (F) Confocal light microscopy of periodontal tissue using a 40 \times objective lens in specimens labelled with calcein green at 48-h intervals in the days prior to sacrifice.

Firmicutes and an increase in Gram negative phyla *Proteobacteria* and *Bacteroidetes* in samples from kidney disease animals as were observed using bacterial culture (Fig. 2D). Corresponding to the described reductions in major taxa and increases in minor ones in kidney disease animals, oral communities from kidney disease animals were found to have higher alpha diversity

when measured using the Simpson Index than communities from control animals (0.75 in controls vs 0.82 in kidney disease, $P = 0.045$).

Ordination plots for all samples revealed that the most significant source of variation was between shipment batches (different batches from the same vendor were used in each experiment).

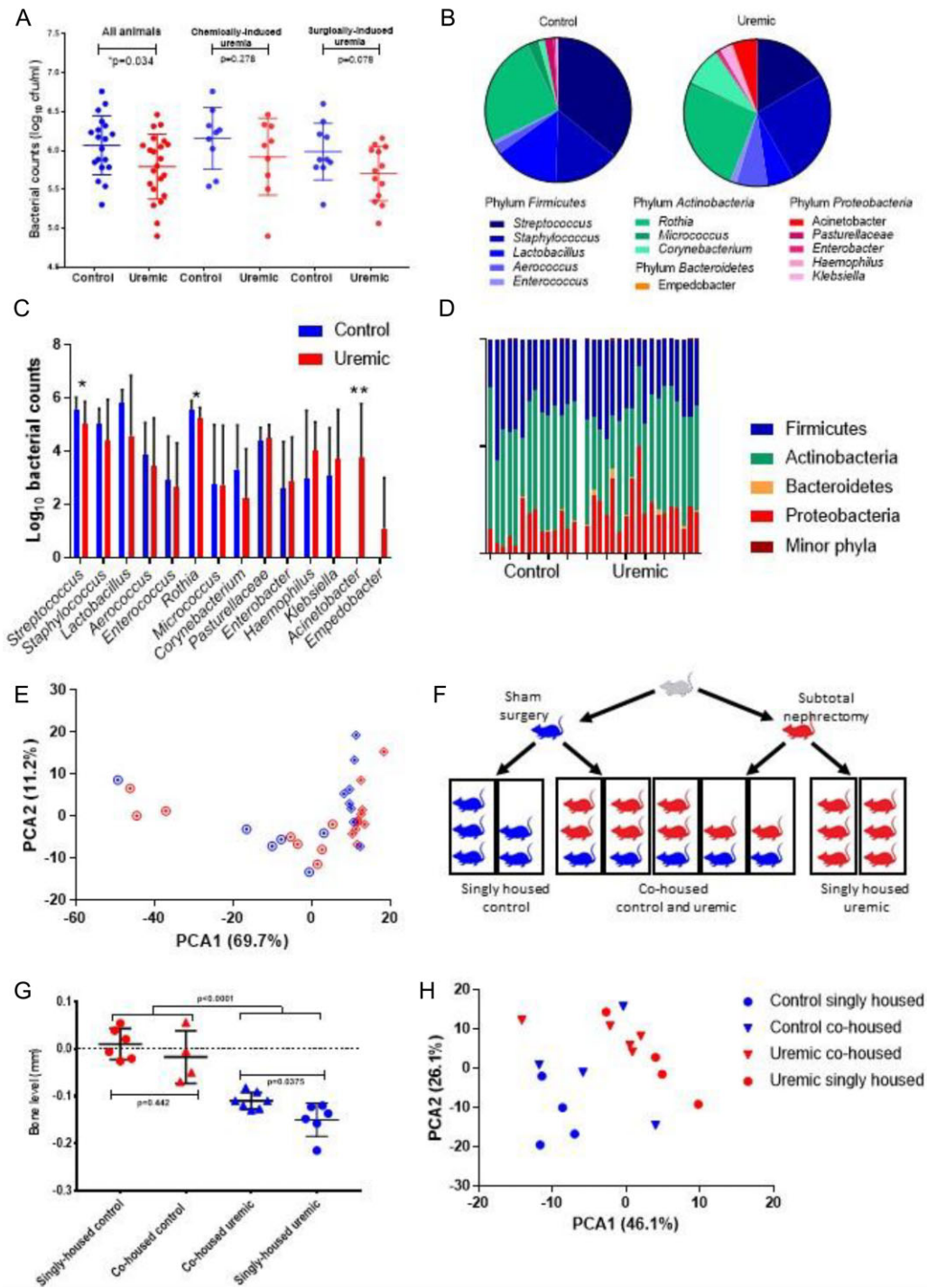


Figure 2: Kidney disease is associated with oral dysbiosis, whilst co-housing alters bacterial communities and affects the severity of periodontal disease. (A) Total bacterial counts (colony forming units/ml) measured by summing colonies counted on blood agar plates grown in aerobic and anaerobic conditions for 48 h. Significance is assessed using Student's *t*-test with Welch's correction for both separate experimental protocols and for the combined dataset. (B) Community composition of the oral microbiota determined by aerobic and anaerobic culture in control and kidney disease rats. All cultured isolates are included, agglomerated to genus level and expressed in terms of their mean percentage contribution to the oral microbial community of each rat. (C) Absolute abundances of each cultured isolate (\log_{10} cfu/ml). Each point describes an individual replicate, significance where shown was calculated using the *t*-test with Welch's correction. * $P < 0.05$. (D) Community composition of the oral microbiota of rats assessed by next generation sequencing of the 16S amplicon. Each vertical bar represents the total microbial community for a single animal, grouped according to experimental conditions (control vs kidney disease), colour is applied according to assigned taxonomy at phylum level. (E) Principal coordinate plot showing distance between oral communities assessed by next generation sequencing of the 16S amplicon. Each point represents the oral community of an individual rat, with symbol shape representing the two experiments performed, which used separate batches of animals (circles denote the chemically induced kidney disease experiment, diamonds surgically induced kidney disease). (F) Housing of animals in the surgically induced arm of the experiment; a total of 13 rats were co-housed, and 11 were singly housed with others of the same treatment protocol. (G) Periodontal bone loss (or lack of bone gain), measured and presented as previously, according to housing for animals in the surgically induced kidney disease experiment. Significance between different groups as shown were calculated by the *t*-test with Welch's correction; analysis by two-way ANOVA is presented in the main text. (H) PCA plot of sequencing data of the oral microbiota of rats in the surgically induced kidney disease experiment, identified according to treatment class (symbol colour) and caging (symbol shape).

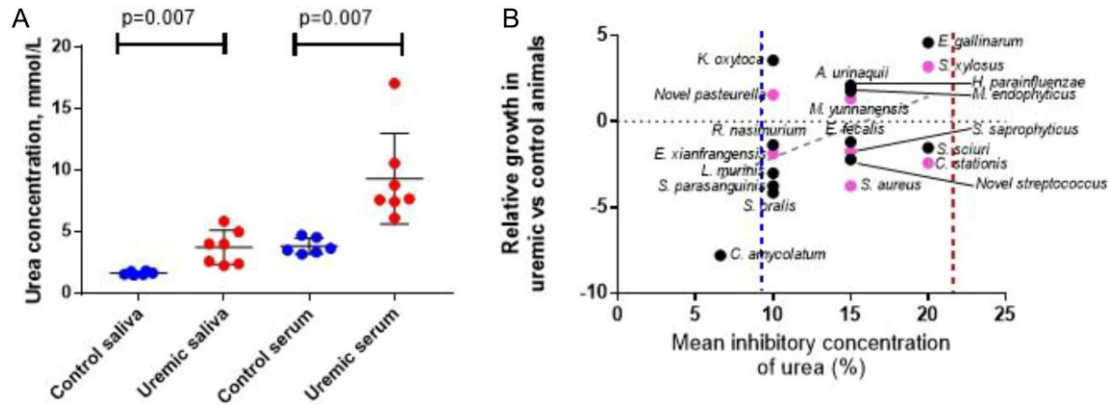


Figure 3: Kidney disease alters salivary biochemistry in rats, which may explain the observed oral dysbiosis. (A) Urea concentration (mmol/L) in induced saliva and serum samples taken at the time of sacrifice in rats after subtotal nephrectomy or sham surgery. Urea concentration was assessed by colorimetric assay and significance was assessed using the t-test with Welch's correction. (B) The mean inhibitory concentration of urea for cultured isolates from the oral microbiota of rats, plotted against their relative growth in kidney disease versus control animals. Each point represents the bacterial species labelled, and the y-axis represents the proportional increase in the mean growth of that species in kidney disease over control animals, with zero representing equal growth in control and kidney disease animals, positive values representing increased growth in kidney disease animals, and negative values representing increased growth in controls. Species demonstrating *in vitro* urease activity are shown in pink. The blue and red dotted lines indicate the mean salivary urea concentrations in control (blue) and kidney disease (red) animals, for comparison purposes.

However, when ordination for each experiment was plotted separately, there was indeed differential clustering between control and kidney disease animals, with ADONIS assessing the significance of separation according to kidney disease proving significant for the surgically induced kidney disease protocol ($R_2 = 0.147$, $P = 0.012$) but not in the chemically induced kidney disease protocol ($R_2 = 0.112$, $P = 0.184$, Fig. 2E).

Co-housing alters bacterial communities and affects the severity of periodontal disease

The surgically induced kidney disease protocol allowed us to investigate the influence of either housing rats singly (with other rats of the same treatment arm; kidney disease with kidney disease or controls with controls), or co-housed (kidney disease with controls, Fig. 2F).

Interestingly, kidney disease animals that were co-housed with controls developed less periodontal bone loss than those housed only with other kidney disease animals (mean bone height -0.149 mm compared to mean of control animals in those that were singly housed, and -0.109 mm in those that were co-housed, $P = 0.038$), implying a protective effect from co-housing with healthy animals. Two-way ANOVA confirmed that whilst treatment class had the biggest effect on bone loss in these animals (accounting for 77% of variance, $P = 0.001$), the contribution of housing also proved significant (6.7% of variance, $P = 0.014$). There was no difference in bone loss between co-housed and singly housed control animals (Fig. 2G).

An ordination plot based on 16S gene sequencing demonstrated that co-housed animals had an intermediate microbial profile between the singly housed control and kidney disease groups (Fig. 2H). Two-way ANOVA carried out for the first two principal components revealed that housing significantly affected clustering in component 2 (19.86% of variance, $P = 0.043$), although to a lesser extent than treatment class (25.84% of variance, $P = 0.024$). Only treatment class significantly affected principal component 1 (treatment 28.48% of variance, $P = 0.0196$; housing 0.02% of variance, $P = 0.94$).

Kidney disease alters salivary biochemistry in rats, which may explain the observed oral dysbiosis

To assess whether alterations in saliva following the induction of kidney disease might be responsible for the differences in oral microbiology, induced saliva samples were obtained using pilocarpine administration to rats under terminal anaesthesia.

There were no differences in either the flow rate or pH of induced saliva (Supplementary data S9); however, kidney disease animals were found to have significantly higher concentrations of salivary urea (in proportion to an increase in serum urea) when measured by colorimetric analysis (1.62 mmol/l in controls vs 3.73 mmol/l in kidney diseases, $P = 0.007$, Fig. 3A).

Untargeted proton nuclear magnetic resonance spectroscopy ($^1\text{H-NMR}$) was performed to characterize biochemical perturbations associated with kidney disease and assess the functionality of the altered microbiota. Salivary concentrations of acetate were 27% lower in kidney disease animals compared with controls (122.19 relative units in controls vs 89.11 in kidney disease, $P = 0.013$), and concentrations of lactate 47% lower (although this did not reach significance, 116.81 vs 61.35 relative units, $P = 0.056$; Supplementary data S10).

In vitro testing was carried out on all bacterial isolates from the cultured analysis that had been deep frozen in pure colonies after initial isolation and identification. There was a positive association between mean growth of bacterial isolates in kidney disease animals and the mean inhibitory concentration for urea (Supplementary data S8). Linear regression was used to calculate a line of best fit, which proved to be significantly different from horizontal (slope 0.34, $P = 0.046$), implying that the higher urea concentrations in saliva from kidney disease animals might be selecting out organisms more able to survive in this environment. Using Christensen's urea agar we assessed the *in vitro* urease activity of all isolates (Fig. 3B); there was a non-significant increase in bacteria demonstrating urease activity in samples from kidney disease animals (urease positive organisms accounting for 14.1% of bacterial growth in kidney disease animals and 8.6% in controls, $P = 0.32$).

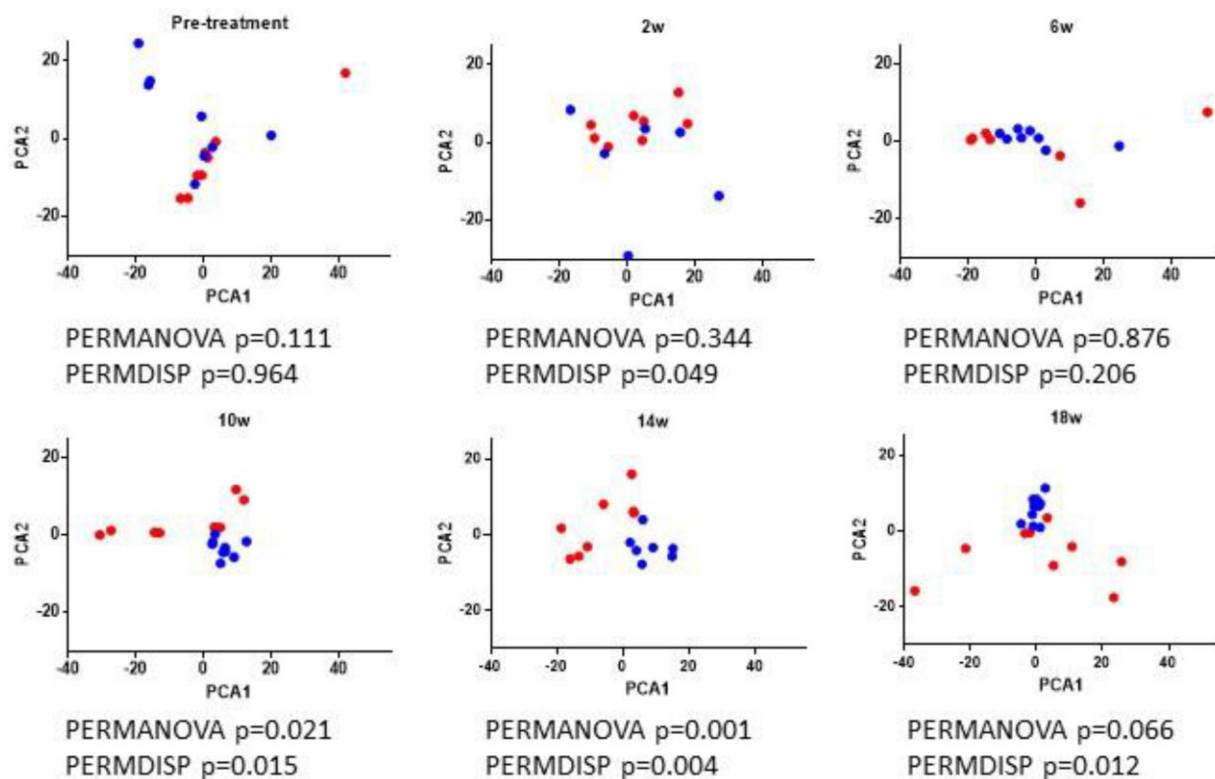


Figure 4: Kidney disease induces progressive oral dysbiosis in mice. Principal component analysis plots of oral microbial communities assessed at four-weekly intervals prior to and after commencing an adenine-containing diet, by next-generation sequencing of the 16S rRNA gene amplicon. Samples from control animals are shown in blue and those from kidney disease animals in red. For each plot the significance is shown for differential clustering (assessed by PerMANOVA) and heterogeneity of variance (assessed by PERMDISP).

Kidney disease induces progressive oral dysbiosis in mice

The method of experimental kidney disease used in the mouse model produces slowly progressive uremia, allowing analysis of the development of dysbiosis over time.

Oral swabs were taken every 4 weeks during the experimental period, and next generation sequencing of the 16S rRNA gene amplicon revealed progressive changes in samples from kidney disease animals, characterized by increased heterogeneity between samples, and progressively differential clustering on principal component analysis (Fig. 4). Significant differences in clustering as measured by PerMANOVA emerged between control and kidney disease microbiotas at 10 weeks into the experimental period (roughly co-incident with the development of significant differences between control and kidney disease animals in weight, suggestive of clinical kidney disease, which first became apparent at 9 weeks into the experimental period, [Supplementary data S2](#)). These changes persisted at 14 weeks, but after 18 weeks of experimental diet, kidney disease animals exhibited such significant within-group differences meaning that although there was still a marked separation between the clustering of kidney disease versus control samples on visual inspection of PCA plots, this did not reach significance when assessed using PerMANOVA ($R^2 = 0.134$, $P = 0.066$). Quantification of population variances using permutational analysis of multivariate dispersions (PERMDISP) confirmed that samples from kidney disease animals became progressively heterogeneous as kidney disease increased (average distances to median being 6.78 in controls and 18.31 in kidney disease by 18 weeks, $P = 0.012$).

The ANalysis of Composition of Microbiomes (ANCOM) methodology was used to identify amplicon sequencing variants (ASVs) that were differentially abundant between groups after correction for multiple hypothesis testing. All ASVs more abundant in controls were from the dominant phylum *Firmicutes*, whilst those increased in kidney disease animals represented a diverse range of organisms from phyla including *Actinobacteria* and *Proteobacteria*, and included ASVs representing organisms (such as from genus *Psychrobacter*) that have previously being implicated in the development of PoD in animals [34].

Periodontal disease can be transmitted by oral microbial transfer into healthy germ-free mice

We further assessed the causative role of bacterial dysbiosis in PoD by carrying out oral microbial transfer (OMT) from control and kidney disease donor mice into germ-free animals (Fig. 5A). The success of OMT was formally assessed by differential clustering on an ordination plot, and using PerMANOVA. This revealed that transfer of the kidney disease microbiota accurately established the donor microbiota in recipient animals (non-significant differences between donors and recipients, $R^2 = 0.12$, $P = 0.158$); that although control recipients visually clustered with control donors, there did exist significant differences between these groups ($R^2 = 0.196$, $P = 0.023$); but that by far the largest differences existed between kidney disease and control recipient microbiotas, similar to the difference between kidney disease and control donors ($R^2 = 0.233$, $P < 0.001$).

Germ-free mice receiving OMT from kidney disease mice developed substantially more periodontal bone loss than those

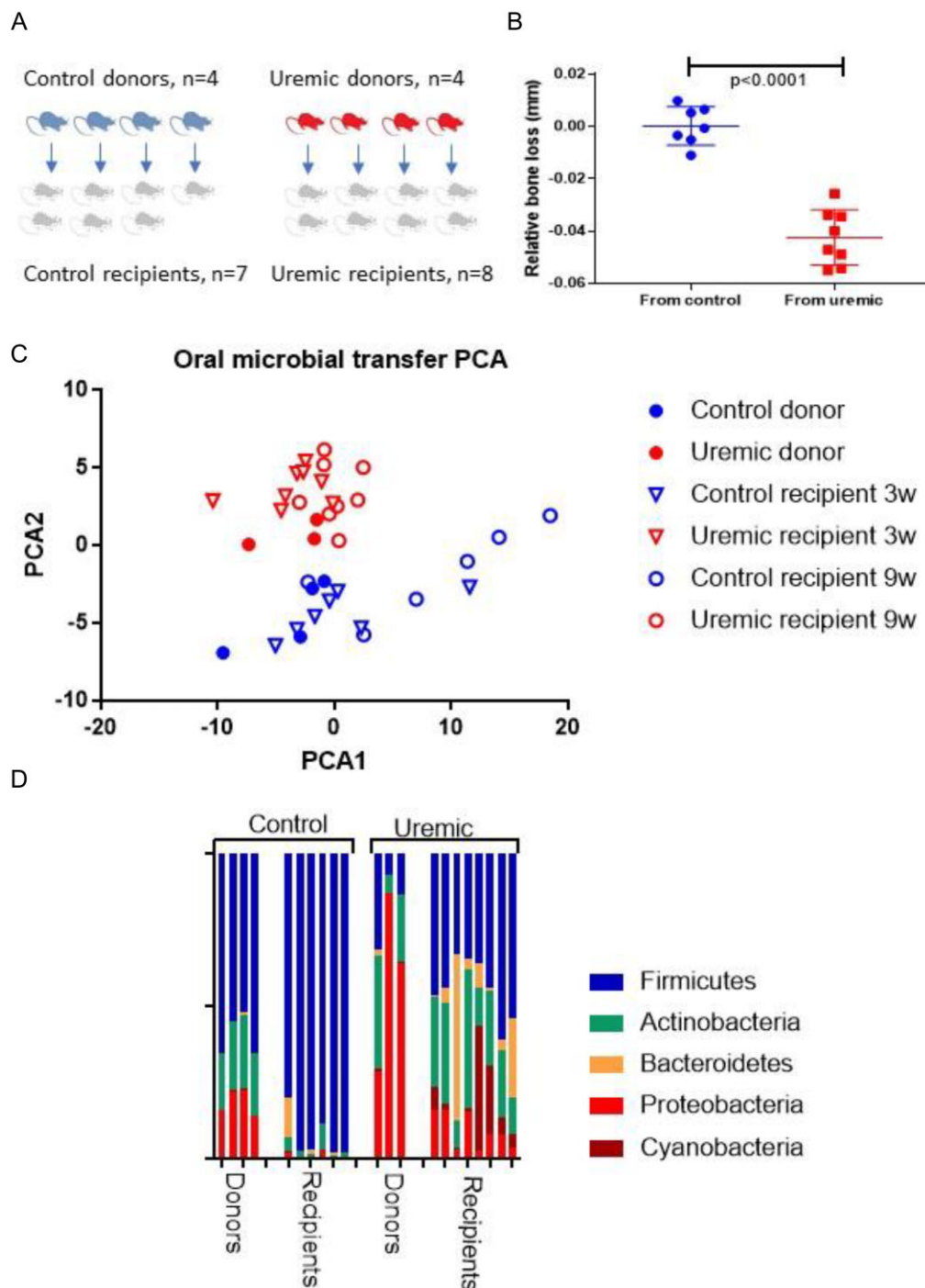


Figure 5: Periodontal disease can be transmitted by oral microbial transfer into healthy germ-free mice. **(A)** Oral microbial communities from four control and four kidney disease donor animals were frozen at the time of sampling and then transferred into germ-free animals at 8 weeks of age. These animals were then conventionally housed, and oral microbial communities were sampled 3 and 9 weeks after transfer, before animals were culled 10 weeks after transfer, at 18 weeks of age. **(B)** Recipients of oral microbiota from kidney disease donors demonstrated significantly more periodontal bone loss than recipients of microbiota from control animals. Each point represents the average periodontal bone loss in a single animal as described in the legend to Fig. 1A. **(C)** Principal component analysis from donor and recipient oral communities. **(D)** Community composition of recipients of oral communities from control and kidney disease donors, assessed by next-generation sequencing of the 16S amplicon at 9 weeks after microbial transfer.

receiving OMT from control mice (-0.042 mm to the mean in control recipients, $P < 0.001$, Fig. 5B and [Supplementary data S11](#)). They were found to have notably dysbiotic oral communities that persisted at 3 and 9 weeks after transfer, and which appeared to represent exaggerations of the features of the control and kidney

disease microbiota seen in both the donor mice and in the previously described rat and mouse experiments. Thus, at 9 weeks, recipients of kidney disease microbiota demonstrated reduced bacterial counts (\log_{10} 6.2cfu/ml in control recipients vs \log_{10} 5.32 in kidney disease recipients, $P < 0.001$), markedly increased alpha

diversity (Simpson Index 0.24 in control recipients vs 0.94 in kidney disease recipients, $P < 0.0001$), and differential clustering on ordination plots, in a similar but more extreme direction to the donor communities (Fig. 5C). Microbiotas from control recipients were heavily dominated by bacteria from phylum *Firmicutes* (with significant cage effects; one group of control recipients were dominated by *Streptococcus* whilst the other was dominated by *Staphylococcus*). Microbiotas from kidney disease recipients displayed heterogeneous oral microbial communities including high prevalence of various phyla including *Firmicutes*, *Actinobacteria*, *Proteobacteria*, *Bacteroidetes*, and *Cyanobacteria* (Fig. 5D).

DISCUSSION

Much of the current literature around the relationship between PoD and CKD centres on the nature of the association: does PoD drive the development of CKD, or does CKD drive the development of PoD, or are there independent causative factors responsible for both?

Here, we demonstrate consistently that both rats and mice with induced kidney disease display a loss of alveolar bone height, implying the high rates of PoD observed in individuals with CKD depend, at least in part, on their kidney disease. We furthermore prove that kidney disease induces consistent patterns of oral bacterial dysbiosis, and show the crucial role of bacteria in the development of PoD through co-caging and microbial transfer experiments: the loss of alveolar bone height is not simply due to the well-described systemic effects of kidney disease on bone. Interestingly, we were unable to demonstrate any evidence of overt inflammation in the gingival tissues, in contrast to other forms of PoD in animal subjects.

The pathophysiology of PoD in human subjects with CKD is poorly described, in particular the role of inflammation in causing bone loss, and we are unaware of any studies describing the histological appearances of PoD in such individuals. However, case series including examination findings in patients with CKD do describe macroscopic features such as gum oedema and contact bleeding, which are consistent with gingival inflammation, and there is also evidence that concentrations of inflammatory cytokines in blood and gingiva-crevicular fluid are higher in CKD patients with periodontal disease than in controls [35, 36]. However, the picture is a complex one: a recent analysis of a large cohort study of patients with both CKD and PoD found a bidirectional relationship between these conditions, which was not explained by inflammation. CKD patients suffering with PoD showing similar concentrations of inflammatory markers including C-reactive protein and serum free light chains compared to those with good oral health, and the authors attributed the association between the conditions to oxidative stress rather than inflammation [37].

The lack of inflammatory response associated with alveolar bone loss in our animal studies is nevertheless a surprise. It might be that PoD in the context of kidney disease represents a spectrum of disease, starting with the reduction we have demonstrated in periodontal bone formation (mediated perhaps by interaction between bacteria in the oral cavity and osteoblasts at the surface of periodontal bone through unknown mechanisms), before progressing to overt inflammatory disease with secondary osteoclastic activity in its later stages. Elsewhere, osteoblastic bone growth has been shown to be inhibited by the presence of bacterial infection following fracture (through the action of cytokine signalling including the IL-1 β /MyD88 pathway [38]), and also by the presence of malignant cells in myeloma (through the action of the

secreted glycoprotein Dickkopf 1 [39]). Alternatively, impaired immune function in kidney disease may dampen the florid inflammation typically seen in aggressive forms of PoD in the general population; it may be that inflammation is a less important factor in PoD in the context of CKD than in other patient groups.

The rats with induced kidney disease in this study did not develop overt hyperparathyroidism (consistent with other studies, which demonstrate that a high phosphorus diet in addition to SNx is required to induce frank hyperparathyroidism in rats [40]), and rates of both incisor dentine formation and bone formation away from the periodontal crest appear to be preserved between control and kidney disease animals. This suggests that the reduced bone formation at the periodontal crest is indeed a localized phenomenon, or perhaps a locally exaggerated form of more widespread skeletal abnormalities present in animals with kidney disease.

A common signature emerged in our experiments of the effects of kidney disease on oral bacterial communities. There was a reduction in overall bacterial counts; an increase in alpha diversity; depletion of taxa such as *Streptococcus* and *Rothia*, which are key components of healthy oral microbiotas [41, 42]; and an increase in bacteria (typically non-oral Gram negative rods) that have previously been associated with PoD [43, 44]. Although the term 'dysbiosis' lacks a formal scientific definition, we believe that the consistent pattern we have described, as well as the association with abnormal bone development, warrants use of the term in this setting. Although few studies in humans have described the oral microbiota in the context of kidney disease, those that have reveal a strikingly similar microbial signature to that observed here. In particular, Hu et al. demonstrated significant changes in oral microbial communities in CKD patients when compared with healthy controls, with an increase in the phylum *Proteobacteria*, at the relative expense, in proportional terms, of taxa in the *Firmicutes* phylum, including *Streptococcus* and *Veillonella* [45]. Kidney transplant recipients with poor graft function [46] and hemodialysis patients [47] have likewise been demonstrated to have dysbiotic oral microbiota, consistent with our assertion that kidney disease itself induces oral dysbiosis.

Increased salivary urea is a possible mechanism driving these changes. The composition of saliva uniquely determines the selective pressures on the oral microbiota, and we showed (notwithstanding the limited correlation of bacterial behaviour in liquid culture compared to *in vivo* biofilms) that there was a correlation between *in vitro* urea tolerance and urease activity and increased growth in kidney disease animals. Notably, *Streptococcus* and *Rothia* isolates, which were present at reduced abundances in kidney disease animals, did not display *in vitro* urease activity and showed reduced tolerance of higher urea concentrations in broth culture.

In this study, kidney disease was not accompanied by a reduction in salivary flow rates and an increase in salivary pH, as described elsewhere in rodent models of kidney disease [48]. The concentration of salivary urea we demonstrated is lower than in the published literature, likely to be a consequence of the mechanism we used to induce saliva, although importantly we show a similar degree of increase in urea concentrations in the saliva of kidney disease animals (roughly double that in controls) as was described elsewhere. Pilocarpine administration overrides physiological control of salivary flow rates, and if the mechanism by which high salivary urea increases pH is dependent on bacterial hydrolysis of urea to ammonium, it is possible that the immediate removal of saliva by pipetting prevented these bacterially mediated effects from taking place. Reduced

concentrations of acetic and lactic acid in kidney disease samples is consistent with the reduction in *Streptococcus* and *Lactobacillus*, which are known to digest sugars and produce a range of organic acids [49].

We carried out two experiments that suggest that oral dysbiosis might be playing a causative role in the loss of periodontal bone height. In the first, co-housing with healthy animals seemed to lessen some of the dysbiotic changes seen in kidney disease animals, and to ameliorate the associated PoD phenotype. It has long been known that co-housing can affect oral microbiology [50], and in work recently published by Abusleme *et al.* it has been shown that healthier microbiota may outcompete and even fully replace more dysbiotic communities [51]. In view of both the co-housing and the oral microbial transfer experiments, it would be interesting in future work to consider whether administration of health-associated species such as *Streptococcus* or *Rothia*, e.g. in oral probiotic mouthwashes, might exert a prophylactic effect against the development of PoD in kidney disease hosts.

In the second experiment, the oral microbial signature of kidney disease that we have described was seen in an exaggerated but stable form when microbiota from control and kidney disease animals were transferred into previously germ-free mice. The ability of abnormal microbial communities to stably establish themselves and cause PoD after transfer into germ-free mice has been previously described [20, 52], and the high degree of periodontal bone loss demonstrated in these animals shows the relevance of oral dysbiosis in the aetiology of periodontal disease. The fact that oral microbiota from kidney disease hosts failed to establish healthy oral communities in healthy recipients may relate as much to depletion of health-associated taxa (such as *Streptococcus*) as to the presence of pathological ones.

A strength of this work is use of several different animal models, which induce different severities and durations of kidney disease and which exclude confounding factors, such as co-morbidity and dental hygiene habits, which may serve as alternative explanations for the high level of PoD in human subjects with CKD [53, 54]. The loss of alveolar bone height we demonstrated in kidney disease animals was less severe than that seen in ligature-induced models of periodontitis in both rats [14] and mice [55]. C57/BL6 mice are known to be relatively resistant to periodontitis; however, the degree of bone loss we demonstrated in kidney disease animals (mean -0.02 mm compared with controls) was similar to that seen in periodontitis models in this strain employing oral gavage with disease-causing micro-organisms such as *Porphyromonas gingivalis* (which variably causes up to 0.03 mm bone loss) [16, 55].

Limitations of this study include use of male animals only (as is common in studies of experimental kidney disease), which may limit generalizability to the whole human CKD population, although population data suggest women with CKD suffer a similar incidence of PoD as men [6]. Apart from parathyroid hormone, we did not assess for other systemic factors that are known to affect bone growth (e.g. serum bicarbonate or serum fibroblast growth factor 23 concentrations); we did not evaluate for evidence of systemic inflammation, or assess for localized inflammation, for instance by examining cytokines in gingivo-crevicular fluid or protein expression in gingival tissue.

Further research could usefully explore the extent to which PoD seen in human populations with CKD is driven by oral dysbiosis as opposed to the systemic biochemical abnormalities well described in CKD mineral and bone disease; it could establish the role of inflammation in the development of the disease, and it could also explore the role of dental screening and

treatment in improving patient outcomes in those with all stages of CKD.

In conclusion, we propose that periodontal disease should be regarded as a novel complication of CKD, and that dysbiotic change in oral bacterial communities induced by the salivary changes present in kidney disease plays a crucial mechanistic role.

SUPPLEMENTARY DATA

Supplementary data are available at [Nephrology Dialysis Transplantation](#) online.

ACKNOWLEDGEMENTS

All experimental work was supported by the Barts and the London Renal Research Fund.

We thank Steve Cannon of the Dental Institute, Queen Mary University of London for his assistance in cutting sections for light microscopy and immunohistochemistry.

We thank Maureen Arora, Dental Physical Sciences, Queen Mary University of London, for her help with the sample preparation for BSE-SEM and CSLM.

We thank Professor William Wade and his research group at the Faculty of Dentistry, Oral, and Craniofacial Sciences, Kings College London for supplying barcoded primers and helping to arrange next-generation sequencing.

We thank Professor Guy Carpenter and Professor Gordon Proctor of the Faculty of Dentistry, Oral, and Craniofacial Sciences, Kings College London for their advice around collection of induced saliva samples in rodents.

We thank Robert Bond and the team at the Biological Research Facility, St Georges University of London for their assistance with the germ-free mouse colony.

We thank Steve Harwood for his support in various aspects of the laboratory work.

FUNDING

The study was supported by the Barts Health renal research fund. No external funding was used.

AUTHORS' CONTRIBUTIONS

Organized according to CRediT taxonomy:

Conceptualization: D.W.R., K.M., M.C., M.M.Y.; Methodology: D.W.R., S.J., D.M., G.R.D., A.B., J.S.; Formal Analysis: D.W.R.; Investigation: D.W.R., A.A., J.K., D.M., A.B.; Resources: J.K., S.J., G.R.D., D.M., A.B., J.S., M.C., M.M.Y.; Data Curation: D.W.R.; Writing—Original draft: D.W.R.; Writing—Review and Editing: All authors; Visualization: D.W.R.; Supervision: K.M., M.C., M.M.Y.; Funding Acquisition: C.T., K.M., M.M.Y.

DATA AVAILABILITY STATEMENT

Raw sequencing data from all samples has been uploaded to the Sequence Read Archive (SRA) of the National Center for Biotechnology Information (NCBI, <https://submit.ncbi.nlm.nih.gov/subs/sra/>). It can be accessed using the accession number **PR-JNA648141**.

All raw NMR data has been uploaded to the Metabolights online repository (<https://ebi.ac.uk/metabolights/>) [56], using the study identifier **MTBLS1833**.

All other raw data, including animal data for the various rodent cohorts and bacteriological data from the culture experiment and *in vitro* microbiological work is available in [supplementary files](#).

Microbiological analysis was carried out in R using packages that are publicly available via CRAN or Github, as detailed earlier in the Methods section.

Analysis of NMR data analysis can be replicated using Matlab scripts in the IMPACT Toolkit developed in house at Imperial College, available from <https://github.com/csmssoftware/IMPACTS>.

CONFLICT OF INTEREST STATEMENT

The authors declare no conflicts of interest.

REFERENCES

- Hajishengallis G, Lamont RJ. Beyond the red complex and into more complexity: the polymicrobial synergy and dysbiosis (PSD) model of periodontal disease etiology. *Mol Oral Microbiol* 2012;**27**:409–19. <https://doi.org/10.1111/j.2041-1014.2012.00663.x>
- Hienz SA, Paliwal S, Ivanovski S. Mechanisms of bone resorption in periodontitis. *J Immunol Res* 2015;**2015**:1. <https://doi.org/10.1155/2015/615486>
- Deschamps-Lenhardt S, Martin-Cabezas R, Hannedouche T et al. Association between periodontitis and chronic kidney disease: systematic review and meta-analysis. *Oral Dis* 2019;**25**:385–402. <https://doi.org/10.1111/odi.12834>
- Chambrone L, Foz AM, Guglielmetti MR et al. Periodontitis and chronic kidney disease: a systematic review of the association of diseases and the effect of periodontal treatment on estimated glomerular filtration rate. *J Clin Periodontology* 2013;**40**:443–56. <https://doi.org/10.1111/jcpe.12067>
- Sharma P, Dietrich T, Sidhu A et al. The periodontal health component of the Renal Impairment In Secondary Care (RI-ISC) cohort study: a description of the rationale, methodology and initial baseline results. *J Clin Periodontology* 2014;**41**:653–61. <https://doi.org/10.1111/jcpe.12263>
- Sharma P, Dietrich T, Ferro CJ et al. Association between periodontitis and mortality in stages 3–5 chronic kidney disease: NHANES III and linked mortality study. *J Clin Periodontology* 2016;**43**:104–13. <https://doi.org/10.1111/jcpe.12502>
- Lertpimonchai A, Rattanasiri S, Tamsailom S et al. Periodontitis as the risk factor of chronic kidney disease: mediation analysis. *J Clin Periodontology* 2019;**46**:631–9. <https://doi.org/10.1111/jcpe.13114>
- Anuradha BR, Katta S, Kode VS et al. Oral and salivary changes in patients with chronic kidney disease: a clinical and biochemical study. *J Indian Soc Periodontol* 2015;**19**:297–301. <https://doi.org/10.4103/0972-124X.154178>
- Lasisi TJ, Raji YR, Salako BL. Salivary creatinine and urea analysis in patients with chronic kidney disease: a case control study. *BMC Nephrol* 2016;**17**:10. <https://doi.org/10.1186/s12882-016-0222-x>
- Martin KJ, González EA. Metabolic bone disease in chronic kidney disease. *J Am Soc Nephrol* 2007;**18**:875–85. <https://doi.org/10.1681/ASN.2006070771>
- Lemesch S, Ribitsch W, Schilcher G et al. Mode of renal replacement therapy determines endotoxemia and neutrophil dysfunction in chronic kidney disease. *Sci Rep* 2016;**6**:34534. <https://doi.org/10.1038/srep34534>
- Randall DW, Kieswich J, Swann J et al. Batch effect exerts a bigger influence on the rat urinary metabolome and gut microbiota than uraemia: a cautionary tale. *Microbiome* 2019;**7**:127. <https://doi.org/10.1186/s40168-019-0738-y>
- Klausen B, Evans RT, Sfintescu C. Two complementary methods of assessing periodontal bone level in rats. *Scand J Dent Res* 1989;**97**:494–9.
- Fernandes MI, Gaio EJ, Oppermann RV et al. Comparison of histometric and morphometric analyses of bone height in ligature-induced periodontitis in rats. *Braz Oral Res* 2007;**21**:216–21. <https://doi.org/10.1590/S1806-83242007000300005>
- Schneider CA, Rasband WS, Eliceiri KW. NIH Image to ImageJ: 25 years of image analysis. *Nat Methods* 2012;**9**:671–5. <https://doi.org/10.1038/nmeth.2089>
- Baker PJ, Dixon M, Roopenian DC. Genetic control of susceptibility to Porphyromonas gingivalis-induced alveolar bone loss in mice. *Infect Immun* 2000;**68**:5864–8. <https://doi.org/10.1128/IAI.68.10.5864-5868.2000>
- Dempster DW, Compston JE, Drezner MK et al. Standardized nomenclature, symbols, and units for bone histomorphometry: a 2012 update of the report of the ASBMR Histomorphometry Nomenclature Committee. *J Bone Miner Res* 2013;**28**:2–17. <https://doi.org/10.1002/jbmr.1805>
- Davis GR, Evershed AN, Mills D. Quantitative high contrast X-ray microtomography for dental research. *J Dent* 2013;**41**:475–82. <https://doi.org/10.1016/j.jdent.2013.01.010>
- Hajishengallis G, Liang S, Payne MA et al. Low-abundance biofilm species orchestrates inflammatory periodontal disease through the commensal microbiota and complement. *Cell Host Microbe* 2011;**10**:497–506. <https://doi.org/10.1016/j.chom.2011.10.006>
- Payne MA, Hashim A, Alsam A et al. Horizontal and vertical transfer of oral microbial dysbiosis and periodontal disease. *J Dent Res* 2019;**98**:1503–10. <https://doi.org/10.1177/0022034519877150>
- Hall TA. BIOEDIT: a user-friendly biological sequence alignment editor and analysis program for WINDOWS 95/98/NT. 1999.
- Huang X, Madan A. CAP3: a DNA sequence assembly program. *Genome Res* 1999;**9**:868–77. <https://doi.org/10.1101/gr.9.9.868>
- Salter SJ, Cox MJ, Turek EM et al. Reagent and laboratory contamination can critically impact sequence-based microbiome analyses. *BMC Biol* 2014;**12**:87. <https://doi.org/10.1186/s12915-014-0087-z>
- Cole JR, Wang Q, Fish JA et al. Ribosomal Database Project: data and tools for high throughput rRNA analysis. *Nucl Acids Res* 2014;**42** (Database issue):D633–42. <https://doi.org/10.1093/nar/gkt1244>
- Kumar S, Stecher G, Li M et al. MEGA X: molecular evolutionary genetics analysis across computing platforms. *Mol Biol Evol* 2018;**35**:1547–9. <https://doi.org/10.1093/molbev/msy096>
- Callahan BJ, McMurdie PJ, Rosen MJ et al. DADA2: high-resolution sample inference from Illumina amplicon data. *Nat Methods* 2016;**13**:581–3. <https://doi.org/10.1038/nmeth.3869>
- Quast C, Pruesse E, Yilmaz P et al. The SILVA ribosomal RNA gene database project: improved data processing and web-based tools. *Nucleic Acids Res* 2013;**41**:D590–6.
- McMurdie PJ, Holmes S. phyloseq: an R package for reproducible interactive analysis and graphics of microbiome census data. *PLoS One* 2013;**8**:e61217. <https://doi.org/10.1371/journal.pone.0061217>
- Revell LJ. phytools: an R package for phylogenetic comparative biology (and other things). *Methods Ecol Evol* 2012;**3**:217–23. <https://doi.org/10.1111/j.2041-210X.2011.00169.x>

30. Silverman JD, Washburne AD, Mukherjee S et al. A phylogenetic transform enhances analysis of compositional microbiota data. *eLife* 2017;**6**. <https://doi.org/10.7554/eLife.21887>
31. Anderson MJ. Distance-based tests for homogeneity of multivariate dispersions. *Biometrics* 2006;**62**:245–53. <https://doi.org/10.1111/j.1541-0420.2005.00440.x>
32. Jari O, Guillaume BF, Michael F et al. vegan: community Ecology Package. <https://cran.r-project.org/web/packages/vegan/index.html>: R package version 2.5-6; 2019 (20 December 2024, date last accessed).
33. Mandal S, Van Treuren W, White RA et al. Analysis of composition of microbiomes: a novel method for studying microbial composition. *Microb Ecol Health Dis* 2015;**26**:27663.
34. Flancman R, Singh A, Weese JS. Evaluation of the impact of dental prophylaxis on the oral microbiota of dogs. *PLoS One* 2018;**13**:e0199676. <https://doi.org/10.1371/journal.pone.0199676>
35. Sun K, Shen H, Liu Y et al. Assessment of alveolar bone and periodontal status in peritoneal dialysis patients. *Front Physiol* 2021;**12**. <https://doi.org/10.3389/fphys.2021.759056>.
36. Ma X, Wang Y, Wu H et al. Periodontal health related-inflammatory and metabolic profiles of patients with end-stage renal disease: potential strategy for predictive, preventive, and personalized medicine. *EPMA Journal* 2021;**12**:117–28. <https://doi.org/10.1007/s13167-021-00239-0>
37. Sharma P, Fenton A, Dias IHK et al. Oxidative stress links periodontal inflammation and renal function. *J Clin Periodontology* 2021;**48**:357–67. <https://doi.org/10.1111/jcpe.13414>
38. Croes M, van der Wal BCH, Vogely HC. Impact of bacterial infections on osteogenesis: evidence from in vivo studies. *J Orthop Res* 2019;**37**:2067–76. <https://doi.org/10.1002/jor.24422>
39. Zhou F, Meng S, Song H et al. Dickkopf-1 is a key regulator of myeloma bone disease: opportunities and challenges for therapeutic intervention. *Blood Rev* 2013;**27**:261–7. <https://doi.org/10.1016/j.blre.2013.08.002>
40. Bajwa NM, Sanchez CP, Lindsey RC et al. Cortical and trabecular bone are equally affected in rats with renal failure and secondary hyperparathyroidism. *BMC Nephrol* 2018;**19**:24. <https://doi.org/10.1186/s12882-018-0822-8>
41. Hyde ER, Luk B, Cron S et al. Characterization of the rat oral microbiome and the effects of dietary nitrate. *Free Radical Biol Med* 2014;**77**:249–57. <https://doi.org/10.1016/j.freeradbiomed.2014.09.017>
42. Sulyanto RM, Thompson ZA, Beall CJ et al. The predominant oral microbiota is acquired early in an organized pattern. *Sci Rep* 2019;**9**:10550. <https://doi.org/10.1038/s41598-019-46923-0>
43. van Winkelhoff AJ, Rurenga P, Wekema-Mulder GJ et al. Non-oral gram-negative facultative rods in chronic periodontitis microbiota. *Microb Pathog* 2016;**94**:117–22. <https://doi.org/10.1016/j.micpath.2016.01.020>
44. Bui FQ, Almeida-da-Silva CLC, Huynh B et al. Association between periodontal pathogens and systemic disease. *Biomed J* 2019;**42**:27–35. <https://doi.org/10.1016/j.bj.2018.12.001>
45. Hu J, Iragavarapu S, Nadkarni GN et al. Location-specific oral microbiome possesses features associated with CKD. *Kidney Int Rep* 2018;**3**:193–204. <https://doi.org/10.1016/j.ekir.2017.08.018>
46. Wu J, Muthusamy A, Al-Ghalith G et al. Comparison of oral microbiome in stable vs declining kidney function in renal transplant recipients [abstract]. *Am J Transplant* 2014;D633–D42. <https://atcmeetingabstracts.com/abstract/comparison-of-oral-microbiome-in-stable-vs-declining-kidney-function-in-renal-transplant-recipients/>
47. Araújo MV, Hong BY, Fava PL et al. End stage renal disease as a modifier of the periodontal microbiome. *BMC Nephrol* 2015;**16**:80. <https://doi.org/10.1186/s12882-015-0081-x>
48. Romero AC, Bergamaschi CT, de Souza DN et al. Salivary alterations in rats with experimental chronic kidney disease. *PLoS One* 2016;**11**:e0148742. <https://doi.org/10.1371/journal.pone.0148742>
49. Nuryana I, Andriani A, Lisdiyanti P et al. Analysis of organic acids produced by lactic acid bacteria. *IOP Conf Ser: Earth Environ Sci* 2019;**251**:012054. <https://doi.org/10.1088/1755-1315/251/1/012054>
50. Caruso R, Ono M, Bunker ME et al. Dynamic and asymmetric changes of the microbial communities after cohousing in laboratory mice. *Cell Rep* 2019;**27**:3401–12.e3. <https://doi.org/10.1016/j.celrep.2019.05.042>
51. Abusleme L, O’Gorman H, Dutzan N et al. Establishment and stability of the murine oral microbiome. *J Dent Res* 2020;**99**:721–9. <https://doi.org/10.1177/0022034520915485>
52. Li B, Ge Y, Cheng L et al. Oral bacteria colonize and compete with gut microbiota in gnotobiotic mice. *Int J Oral Sci* 2019;**11**:10. <https://doi.org/10.1038/s41368-018-0043-9>
53. Akar H, Akar GC, Carrero JJ et al. Systemic consequences of poor oral health in chronic kidney disease patients. *Clin J Am Soc Nephrol* 2011;**6**:218–26. <https://doi.org/10.2215/CJN.05470610>
54. Hou Y, Wang X, Zhang CX et al. Risk factors of periodontal disease in maintenance hemodialysis patients. *Medicine (Baltimore)* 2017;**96**:e7892. <https://doi.org/10.1097/MD.0000000000007892>
55. Marchesan J, Girmay MS, Jing L et al. An experimental murine model to study periodontitis. *Nat Protoc* 2018;**13**:2247–67. <https://doi.org/10.1038/s41596-018-0035-4>
56. Haug K, Cochrane K, Nainala VC et al. MetaboLights: a resource evolving in response to the needs of its scientific community. *Nucleic Acids Res* 2020;**48**:D440–d4.